

# Mathematical modeling of hepatocellular carcinoma incorporating immunotherapy

Edna Chilenje Manda<sup>1,\*</sup>, Faraimunashe Chirove<sup>2</sup>

<sup>1</sup>Department of Mathematics and Statistics, Mzuzu University, Malawi

manda.ec@mzuni.ac.mw  0000-0001-9970-3707

<sup>2</sup>University of Johannesburg, Johannesburg, South Africa

fchirove@uj.ac.za  0000-0001-6820-688X

Received: August 10, 2023, Accepted: November 25, 2024, Published: December 23, 2024

**Abstract:** We develop a within-host mathematical model for hepatitis B virus infection that leads to hepatocellular carcinoma incorporating immunotherapy as an intervention strategy and also demonstrating drug effects in the sub-therapeutic, therapeutic and toxicity regions of concentration. The model includes the dynamics of hepatocytes, immune cells, cytokines and hepatitis B virus dynamics using a system of ordinary differential equations. Model parameters were estimated using the flexible modeling environment algorithm. Treatment was presented replicating realistic pharmacokinetics of a drug called Nivolumab as a monoclonal antibody type of immunotherapy. Results suggests that immunotherapy reduces the growth of cancer cells when the drug concentration is in a therapeutic region but complete eradication is not possible. Drug concentration above the therapeutic region reduced the cancer cells to better levels but this benefit is associated with toxicity of the drug. Drug concentration below the therapeutic region is associated with little reduction in cancer cells.

**Keywords:** hepatocytes, pharmacokinetics, cytokines, immunotherapy

## I. INTRODUCTION

Hepatocellular carcinoma (HCC) is the fifth most common cancer and the third leading cause of cancer-related deaths worldwide [1]. The incidence and mortality associated with HCC increase each year due to either hepatitis C virus (HCV) or hepatitis B virus (HBV) with about 80% cases of HCC associated with chronic

hepatitis B virus (HBV) [2, 3]. In this study we will focus on HBV related HCC.

Most therapeutic options have either failed or performed poorly in treating HCC cases. Immunotherapy is a recent approach used in treating advanced HCC [4,5]. Immunotherapy uses substances made by the body or in the lab to restore immune system function in people with liver cancer. It stops or slows the growth of cancer cells, stops cancer from spreading to other parts of the body and also helps the immune system work better at destroying cancer cells [6]. There are different types of immunotherapy such as monoclonal antibodies, checkpoint inhibitors, cancer vaccines, oncolytic viruses and cytokines to mention a few. Monoclonal antibodies are one of the effective immunotherapy strategies used which reduce the growth of cancer cells. Nivolumab is an example of a monoclonal antibody immunotherapy drug used for the treatment of HCC. Nivolumab is administered as an intravenous (IV) infusion every 2 weeks at a dose of 240 mg/kg [7, 8]. We shall use Nivolumab to illustrate the benefits of immunotherapy in our current study [9, 10]. Even though all the mentioned immunotherapy types can be captured in a mathematical model, we shall subject our current study to illustrate the benefits of monoclonal antibodies.

The immune system is the body's defense against infectious organisms and is capable of recognizing and eliminating tumour cells, although cancer cells are con-

**Copyright:** © 2024 Edna Chilenje Manda, Faraimunashe Chirove. This article is distributed under the terms of the Creative Commons Attribution License (CC BY 4.0), which permits unrestricted use, distribution, and reproduction in any medium, provided the original author and source are credited. \*Corresponding author

**Citation:** Edna Chilenje Manda, Faraimunashe Chirove, Mathematical modeling of hepatocellular carcinoma incorporating immunotherapy, Biomath 13 (2024), 2411256, <https://doi.org/10.55630/j.biomath.2024.11.256> 1/19

sidered poorly immunogenic [11]. Evidence available suggests that immune cells can play a crucial role in the control of cancer. Experimentally, animal models exhibited tumour immunity in several animal models. The immune system also recognizes the presence of tumours through accumulation of immune cells at tumour sites [12, 13]. HBV infection also activates cytokines which are a category of small proteins that are important in cell signalling and are activated due to infection. Their activation is also linked to immune system cells. The cytokines associated with the advanced stage of HBV infection that leads to HCC are the inhibitory cytokines, the pro-inflammatory cytokines, and the anti-inflammatory cytokines [14]. Our study shall capture the use of generic cytokines categories without mentioning the specific cytokines involved. However, the effects of the specific cytokines in each category can easily be adapted to model design in this study.

The aim of this study is to design a mathematical model to demonstrate the pharmacokinetic effects of immunotherapy as an intervention strategy for HCC. The paper is organized as follows: model formulation in Section II, the model’s mathematical analysis in Section III, numerical simulations in Section IV and discussion of results and conclusion in Section V.

## II. THE MATHEMATICAL MODEL

We formulate a model that incorporates hepatocytes dynamics, hepatitis B virus dynamics, immune system cells dynamics, cytokine dynamics and cancer cells dynamics.

### A. Hepatocytes dynamics

The dynamics of the hepatocytes populations are given by the following equations:

$$\frac{dH}{dt} = \pi - (\beta(C + \eta_3 I_{cr} + \eta_2 I_{ci} + \eta_1 H_B^e) + \mu)H, \tag{1}$$

$$\begin{aligned} \frac{dI_{cr}}{dt} = & \lambda H - \delta_r \frac{H_B^{i2}}{H_B^{i2} + (N_1 I_{cr})^2} \left( \frac{c_a}{I_a + c_a} \right) I_{cr} \\ & - \left( \mu + \zeta + \phi_1 \left( \frac{H_B^i}{H_B^i + c} \right) + \gamma T_c \left( \frac{c_i}{c_i + I_i} \right) \right) I_{cr}, \end{aligned} \tag{2}$$

$$\begin{aligned} \frac{dI_{ci}}{dt} = & \zeta I_{cr} - \delta_i \frac{H_B^{i2}}{H_B^{i2} + (N_2 I_{ci})^2} \left( \frac{c_a}{I_a + c_a} \right) I_{ci} \\ & - \left( \mu + \phi_2 \left( \frac{H_B^i}{H_B^i + c} \right) + \gamma T_c \left( \frac{c_i}{c_i + I_i} \right) \right) I_{ci}. \end{aligned} \tag{3}$$

The healthy hepatocytes regenerate from a source outside the liver [15] at a rate  $\pi$ . They are removed out of their class either through natural death at a rate  $\mu$  or through infection by the infected hepatocytes in the chronic phase, infected hepatocytes in the cirrhotic phase, the cancer cells [16] and the external hepatitis B virus according to a mass action infection term  $\lambda = \beta(C + \eta_3 I_{cr} + \eta_2 I_{ci} + \eta_1 H_B^e)$  since the rate of infection increases with the increase in contact. The parameter  $\beta$  is the rate that contact between a healthy hepatocyte ( $H$ ), and either the infected hepatocytes in the chronic phase,  $I_{cr}$  the infected hepatocytes in the cirrhotic phase,  $I_{ci}$  the external hepatitis B virus  $H_B^e$  or the cancer cells  $C$  results in a successful infection.

The rates of infection by these infectious classes differ due to the fact that during liver cancer, there are more cancer cells circulating followed by the external hepatitis B virus, then the infected hepatocytes in the chronic phase and the infected hepatocytes in the cirrhotic phase. We account for the differences in infection by introducing dimensionless parameters  $\eta_1$ ,  $\eta_2$  and  $\eta_3$  which are related by  $0 < \eta_2 < \eta_1 < \eta_3 < 1$ . When the healthy hepatocytes cells are infected, they change their status to become infected hepatocytes in the chronic phase  $I_{cr}$ .

The infected hepatocytes in the chronic phase  $I_{cr}$  are removed from their class either by natural death at a rate  $\mu$  or by repeated infection by the internal virus that leads to formation of cancer cells at a rate  $\phi_1$  or production of free virions at a rate  $\delta_r$  due to bursting of  $I_{cr}$  which is presented by logistic hill kinetics and is slowed down by the anti-inflammatory cytokines.

The HBV inside the  $I_{cr}$  is killed by HBV specific cytotoxic T lymphocytes at a rate  $\gamma$  [17]. This mortality is amplified by inflammation responses within the liver facilitated by the antiviral cytokines which inhibit the viral replication. The killing of the intracellular hepatitis B inside the  $I_{cr}$  is suppressed by the inhibitory cytokines [18]. Continued inflammation of  $I_{cr}$  progresses to infected hepatocytes in the cirrhotic phase  $I_{ci}$  at a rate  $\zeta$ . They are removed out of their class by natural death a rate  $\mu$ , killing by cytotoxic T lymphocytes at a rate  $\gamma$ , a process inhibited by inhibitory cytokines, bursting to produce free virions at a rate  $\delta_i$  which follows a logistic hill kinetics which is slowed down by the anti-inflammatory cytokines and by repeated infection by the internal hepatitis B virus that leads to scarring of the  $I_{ci}$ ’s which eventually leads to formation of cancer cells at a rate  $\phi_2$  [19]. The parameters  $c_a$  and  $c_i$  are the saturation constant for the antiviral cytokines and inflammatory cytokines respectively.

**B. Hepatitis B virus dynamics**

The dynamics of the internal and external hepatitis B viruses are given by the following equations:

$$\begin{aligned} \frac{dH_B^i}{dt} = & \alpha H_B^i \left(1 - \frac{H_B^{i2}}{H_B^{i2} + (N_1 I_{cr})^2}\right) \\ & + \alpha_1 H_B^i \left(1 - \frac{H_B^{i2}}{H_B^{i2} + (N_2 I_{ci})^2}\right) \\ & - \delta_r N_1 I_{cr} \frac{H_B^{i2}}{H_B^{i2} + (N_1 I_{cr})^2} \\ & - \delta_i N_2 I_{ci} \frac{H_B^{i2}}{H_B^{i2} + (N_2 I_{ci})^2} - \mu_v H_B^i, \end{aligned} \quad (4)$$

$$\begin{aligned} \frac{dH_B^e}{dt} = & \delta_r N_1 I_{cr} \frac{H_B^{i2}}{H_B^{i2} + (N_1 I_{cr})^2} \\ & + \delta_i N_2 I_{ci} \frac{H_B^{i2}}{H_B^{i2} + (N_2 I_{ci})^2} - \mu_v H_B^e. \end{aligned} \quad (5)$$

The internal virus inside the  $I_{cr}$  and  $I_{ci}$  grow at maximum rates of  $\alpha$  and  $\alpha_1$  respectively and is reduced by a logistic Hill kinetics with a parameter depending on the maximum carrying capacity of  $N_1$  and  $N_2$  viruses in the  $I_{cr}$  and the  $I_{ci}$  respectively. We use the Hill equation as it is related to the logistic function if plotted on a log scale [20].  $N_1$  and  $N_2$  are the average number of viruses produced by each  $I_{cr}$  and  $I_{ci}$  respectively. The internal virus  $H_B^i$  is lost either due to the bursting of  $I_{cr}$  at a rate  $\delta_r$  or  $I_{ci}$  at a rate  $\delta_i$  or due to its own natural death at a rate  $\mu_v$ .

The external hepatitis B virus  $H_B^e$  populations increase when the  $I_{cr}$  and  $I_{ci}$  burst and release the virus that they contain at burst rates  $\delta_r$  and  $\delta_i$  respectively. The reduction of the external virus is due to natural death at a rate of  $\mu_v$ .

**C. Immune cells dynamics**

The dynamics of the immune cells are given by the following equations:

$$\frac{dT_4}{dt} = \pi_4 - \left(\frac{\phi_4 I_p}{I_p + c_p}\right) T_4 - \mu_4 T_4, \quad (6)$$

$$\frac{dT_2}{dt} = \left(\frac{\phi_4 I_p}{I_p + c_p}\right) T_4 - \mu_4 T_2, \quad (7)$$

$$\frac{dT_8}{dt} = \pi_8 - \left(\frac{\phi_8 I_p}{I_p + c_p}\right) T_8 - \mu_8 T_8, \quad (8)$$

$$\frac{dT_c}{dt} = \left(\frac{\phi_8 I_p}{I_p + c_p}\right) T_8 - \mu_8 T_c. \quad (9)$$

Production of the CD4<sup>+</sup>T-cells,  $T_4$  is in the thymus at a rate  $\pi_4$  and their loss is through activation by the pro-inflammatory cytokines to become  $T_2$  helper cells at a rate  $\phi_4$  [21] and also natural death at a rate  $\mu_4$ .

The parameter  $c_p$  is the saturation constant for the pro-inflammatory cytokines. The  $T_2$  helper cells get their source from activated  $T_4$  cells at a rate  $\phi_4$  and die at a rate  $\mu_4$ . The CD8<sup>+</sup>T-cells,  $T_8$  are developed in the bone marrow and thymus at a rate of  $\pi_8$  and after an HBV infection has occurred, the HBV specific CD8<sup>+</sup>T-cells become activated by pro-inflammatory cytokines to become cytotoxic CD8<sup>+</sup>T-cells,  $T_c$  [22]. The  $T_8$  and  $T_c$  cells die at a rate  $\mu_8$ .

**D. Cancer cells dynamics**

The growth of many organisms under normal conditions follow the universal law [23, 24] that states that the total body mass  $m$  grows with a rate  $am^p(1 - (\frac{m}{M_0})^{1-p})$ , where the exponent  $p \approx \frac{3}{4}$ ,  $a$  is the growth rate and  $M_0$  is the maximum size of the organism. The same studies have shown that cancer cell growth can be described similarly. In this study, we adopt this description to model the growth of cancer cells. The dynamics of the cancer cells are governed by two processes; intrinsic growth of the cancer cells and elimination due to the cytotoxic CD8<sup>+</sup>T-cells.

$$\begin{aligned} \frac{dC}{dt} = & \left(\pi_c + (\phi_1 I_{cr} + \phi_2 I_{ci}) \left(\frac{H_b^i}{H_b^i + c}\right)\right) C^{\frac{3}{4}} \\ & \times \left(1 - \left(\frac{C}{C_0}\right)^{\frac{1}{4}}\right) - \gamma T_c \left(\frac{c_i}{c_i + I_i}\right) C. \end{aligned} \quad (10)$$

In Equation (10), the cancer cells grow either at a rate  $\pi_c$  or due to  $I_{cr}$  and  $I_{ci}$  which develop into cancer cells due to repeated infection by the internal hepatitis B virus. The parameter  $C_0$  is the maximum size of the cancer cells and  $C$  is the total body mass of the cancer cells. The cancer cells are killed by the cytotoxic CD8<sup>+</sup>T-cells,  $T_c$  at a rate  $\gamma$ . The inhibitory cytokines reduce the killing ability of the cytotoxic cells in killing the cancer cells and we assume the rate of removal of cancer cells to be a decreasing function of the inhibitory cytokines [25]. The parameter  $c_i$  is the saturation constant of the inhibitory cytokines.

**E. Cytokine dynamics**

The dynamics of the cytokines is given by the following equations:

$$\frac{dI_i}{dt} = \pi_i T_2 - (k_r I_{cr} + k_i I_{ci} + k_c C) I_i - \mu_i I_i, \quad (11)$$

$$\frac{dI_p}{dt} = \pi_p T_4 - (k_4 T_4 + k_8 T_8) I_p - \mu_p I_p, \quad (12)$$

$$\frac{dI_a}{dt} = \pi_a T_8 - (\nu_r I_{cr} + \nu_i I_{ci}) I_a - \mu_a I_a. \quad (13)$$

We assume that the inhibitory cytokines,  $I_i$  are produced by the  $T_2$  cells at a rate of  $\pi_i$  and undergo

natural decay at a rate of  $\mu_i$ . The inhibitory cytokines are also lost during inhibition of the  $I_{cr}$ , the  $I_{ci}$  and the cancer cells at rates  $k_r$ ,  $k_i$ , and  $k_c$  respectively. The pro-inflammatory cytokines,  $I_p$  are produced by the  $T_4$  cells at a rate  $\pi_p$  and are removed out of their class either through natural decay a rate  $\mu_p$  or when they activate  $T_4$  and  $T_8$  cells at rates  $k_4$  and  $k_8$  respectively. The anti-inflammatory cytokines,  $I_a$  are produced by the  $T_8$  cells at a rate  $\pi_a$  and undergo natural decay at a rate of  $\mu_a$ . The anti-inflammatory cytokines are also lost during inhibition of the viral replication in the  $I_{cr}$  and  $I_{ci}$  at rates  $\nu_r$  and  $\nu_i$  respectively. Figure 1 shows the interactions explained in model formulation.

F. The reduced model

Cancer growth involves multiple time scales. The growth of cancer cells occurs on a timescale of months to years in vivo and weeks to months in vitro [26], the recruitment of hepatocytes and immune cells occurs on a time scale of days to weeks and the secretion and decay of cytokines occur on a time scale of seconds to hours [24]. To understand the dynamics of cancer growth, we simplify our model using quasi-steady-state approximations for the cytokine concentration. Under these assumptions equations (11) – (13) become

$$I_i = \frac{\pi_i T_2}{(k_r I_{cr} + k_i I_{ci} + k_c C) + \mu_i}, \tag{14}$$

$$I_p = \frac{\pi_p T_4}{(k_4 T_4 + k_8 T_8) + \mu_p}, \tag{15}$$

$$I_a = \frac{\pi_a T_8}{(\nu_r I_{cr} + \nu_i I_{ci}) + \mu_a}. \tag{16}$$

Evidence indicates that the immune cells do not get infected during growth of cancer cells [27, 28]. It is reasonable to assume that the immune cells are always at the adequate required levels at all time. We can achieve this by also using the quasi-steady state approximations for immune cells concentration. Adding equations (6) – (7) for the CD4<sup>+</sup>T cells and letting  $T = T_4 + T_2$  and adding equations (8) – (9) for the CD8<sup>+</sup>T cells and letting  $T_0 = T_8 + T_c$  we obtain

$$T = \frac{\pi_4}{\mu_4} \quad \text{and} \quad T_0 = \frac{\pi_8}{\mu_8}. \tag{17}$$

Substituting equations (17) into equations (14) – (16), we obtain

$$I_i = \frac{a_0}{(k_r I_{cr} + k_i I_{ci} + k_c C) + \mu_i}, \tag{18}$$

$$I_p = \frac{\pi_p \pi_4 \mu_8}{k_4 \pi_4 \mu_8 + k_8 \pi_8 \pi_4 + \mu_p \mu_4 \mu_8}, \tag{19}$$

$$I_a = \frac{a_1}{(\nu_r I_{cr} + \nu_i I_{ci}) + \mu_a}, \tag{20}$$

where expressions  $a_0$  and  $a_1$  are given in the Appendix. Substituting equations (18) – (20) into equations (1) – (5) and (10), the model is then simplified to a system of six equations,

$$\frac{dH}{dt} = \pi - (\lambda + \mu)H, \tag{21}$$

$$\begin{aligned} \frac{dI_{cr}}{dt} = & \lambda H - \left( \mu + \zeta + \phi_1 \left( \frac{H_B^i}{H_B^i + c} \right) + \xi_3 \right) I_{cr} \\ & - \delta_r \frac{H_B^{i2}}{H_B^{i2} + (N_1 I_{cr})^2} \xi_1 I_{cr}, \end{aligned} \tag{22}$$

$$\begin{aligned} \frac{dI_{ci}}{dt} = & \zeta I_{cr} - \left( \mu + \phi_2 \left( \frac{H_B^i}{H_B^i + c} \right) + \xi_3 \right) I_{ci} \\ & - \delta_i \frac{H_B^{i2}}{H_B^{i2} + (N_2 I_{ci})^2} \xi_1 I_{ci}, \end{aligned} \tag{23}$$

$$\begin{aligned} \frac{dH_B^i}{dt} = & \alpha H_B^i \left( 1 - \frac{H_B^{i2}}{H_B^{i2} + (N_1 I_{cr})^2} \right) \\ & + \alpha_1 H_B^i \left( 1 - \frac{H_B^{i2}}{H_B^{i2} + (N_2 I_{ci})^2} \right) - \mu_v H_B^i \\ & - N_1 \delta_r I_{cr} \frac{H_B^{i2}}{H_B^{i2} + (N_1 I_{cr})^2} \\ & - N_2 \delta_i I_{ci} \frac{H_B^{i2}}{H_B^{i2} + (N_2 I_{ci})^2}, \end{aligned} \tag{24}$$

$$\begin{aligned} \frac{dH_B^e}{dt} = & \delta_r N_1 I_{cr} \frac{H_B^{i2}}{H_B^{i2} + (N_1 I_{cr})^2} \\ & + \delta_i N_2 I_{ci} \frac{H_B^{i2}}{H_B^{i2} + (N_2 I_{ci})^2} - \mu_v H_B^e, \end{aligned} \tag{25}$$

$$\begin{aligned} \frac{dC}{dt} = & \left( \pi_c + (\phi_1 I_{cr} + \phi_2 I_{ci}) \left( \frac{H_B^e}{H_B^e + c} \right) \right) C^{\frac{3}{4}} \\ & \times \left( 1 - \left( \frac{C}{C_0} \right)^{\frac{1}{4}} \right) - \xi_3 C, \end{aligned} \tag{26}$$

where

$$\begin{aligned} \xi_1 = & \frac{a_1 + c_a (\nu_r I_{cr} + \nu_i I_{ci} + \mu_a)}{c_a (\nu_r I_{cr} + \nu_i I_{ci} + \mu_a)}, \\ \xi_3 = & \frac{a_3 c_i (k_r I_{cr} + k_i I_{ci} + k_c \mu_i C) + a_0}{c_i (k_r I_{cr} + k_i I_{ci} + k_c C + \mu_i)}. \end{aligned}$$

III. THE MATHEMATICAL ANALYSIS

A. Feasible region

The model examines the dynamics of the cell populations, therefore we require all the parameters and state variables to be non-negative. We will therefore analyze the model in a possible feasible region  $\Omega$ .

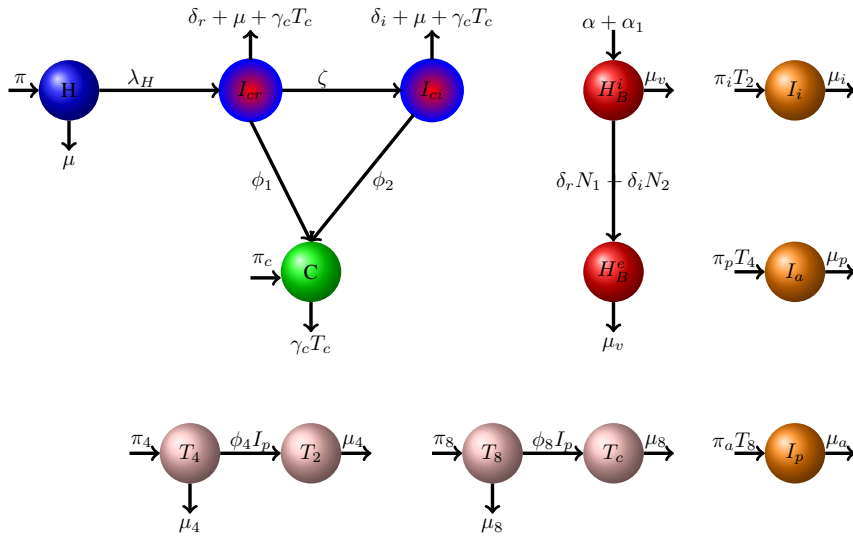


Fig. 1: Model diagram.

$$\Omega = \left\{ (H, I_{cr}, I_{ci}, H_B^i, H_B^e, C) \in \mathbb{R}_+^6 : H_{tot} \leq \frac{\pi}{\mu}, \right. \\ \left. H_{Btot} \leq \frac{\alpha + \alpha_1}{\mu_v}, C \leq \left( \frac{m}{C_0^{-\frac{1}{4}} m - m_1} \right)^4 \right\},$$

where  $H_{tot} = H + I_{cr} + I_{ci}$  and  $H_{Btot} = H_B^i + H_B^e$ .

**Lemma 1.** *Let  $H(0) \geq 0$ ,  $I_{cr}(0) \geq 0$ ,  $I_{ci}(0) \geq 0$ ,  $H_B^e(0) \geq 0$ ,  $H_B^i(0) \geq 0$  and  $C(0) \geq 0$ . Then the solutions of  $H(t)$ ,  $I_{cr}(t)$ ,  $I_{ci}(t)$ ,  $H_B^e(t)$ ,  $H_B^i(t)$ , and  $C(t)$ , are positively invariant for all  $t \geq 0$  in the region  $\Omega$ .*

To prove positivity, we need to ensure that the state variables remain non-negative and solutions of the system remain positive for all  $t \geq 0$  given positive initial conditions. The proof has been omitted in the manuscript because it is standard and easy to show.

Next we prove boundedness.

*Proof:* Summing the populations from equations (21) – (23), we obtain  $\frac{dH_{tot}}{dt} \leq \pi - \mu H_{tot}$ , this yields  $H_{tot} \leq \frac{\pi}{\mu} = H_0$ , and taking the limit supremum of  $H_{tot}$  as  $t \rightarrow \infty$ , we obtain  $\lim_{t \rightarrow \infty} \sup H_{tot}(t) \leq H_0$ .

Summing equations (24) – (25), we obtain  $\frac{dH_{Btot}}{dt} \leq \alpha + \alpha_1 - \mu_v H_{Btot}$ , this yields  $H_{Btot} \leq \frac{\alpha + \alpha_1}{\mu_v} = B_0$ , and taking the limit supremum of  $H_{Btot}$  as  $t \rightarrow \infty$ , we obtain  $\lim_{t \rightarrow \infty} \sup H_{Btot}(t) \leq B_0$ .

From Equation (26) we have:

$$\frac{dC}{dt} \leq C \left( \frac{m}{C^{\frac{1}{4}}} - \frac{m}{C_0^{\frac{1}{4}}} - m_1 \right), \\ m = \pi_c + H_0(\phi_1 + \phi_2) \left( \frac{B_0}{B_0 + c} \right), \\ m_1 = \frac{a_3 c_i H_0 (k_r + k_i) + a_0}{c_i (H_0 (k_r + k_i) + \mu_i)}.$$

Then,

$$\frac{dC}{dt} \leq C^{1-\frac{1}{4}} m - C C_0^{-\frac{1}{4}} m - C m_1, \\ \frac{dC}{dt} \leq C^{\frac{3}{4}} m - C \left( C_0^{-\frac{1}{4}} m - m_1 \right), \\ \frac{dC}{dt} + C \left( C_0^{-\frac{1}{4}} m - m_1 \right) \leq C^{\frac{3}{4}} m. \quad (27)$$

From the Bernoulli equation (27), let  $g = C_0^{-\frac{1}{4}} m - m_1$ ,  $U = C^{\frac{1}{4}}$ , therefore  $C = U^4$  and  $\frac{dC}{dt} = 4U^3 \frac{dU}{dt}$ . Substituting in equation (27) and dividing through by  $4U^3$  gives a linear equation in  $U$ :

$$\frac{dU}{dt} + \frac{gU}{4} \leq \frac{m}{4} \quad (28)$$

Using the integrating factor (IF) method,  $p(t) = \frac{g}{4}$ ,  $IF = \exp\left(\frac{g}{4}t\right)$  and multiplying equation (28) by the IF and integrating, we get:

$$\exp\left(\frac{g}{4}t\right)U \leq \frac{m}{g} \exp\left(\frac{g}{4}t\right) + K, \\ U \leq \frac{m}{g} + K \exp\left(-\frac{g}{4}t\right),$$

where  $K$  is constant of integration. We have  $U = C^{\frac{1}{4}}$ , hence:

$$C^{\frac{1}{4}} \leq \frac{m}{g} + K \exp\left(-\frac{g}{4}t\right),$$

$$C(t) \leq \left(\frac{m}{g} + K \exp\left(-\frac{g}{4}t\right)\right)^4.$$

Thus we have,

$$C(t) \leq \left(\frac{m}{C_0^{-\frac{1}{4}}m - m_1} + K \exp\left(-\frac{C_0^{-\frac{1}{4}}m - m_1}{4}t\right)\right)^4$$

Therefore,

$$\limsup_{t \rightarrow \infty} C(t) \leq \left(\frac{m}{C_0^{-\frac{1}{4}}m - m_1}\right)^4.$$

Therefore,  $C(t)$  is bounded. ■

Since all state variables are positive and bounded in  $\mathbb{R}_+^6$ , then the region  $\Omega$  is a feasible region for our model.

### B. The reproduction number

We computed  $R_0$ , using the next generation matrix method used in Watmough and Van Den Driessche [29]. The details of the computations are quite standard and we leave them out of this manuscript and only give the final next generation matrix  $FV^{-1}$ .

$$FV^{-1} = \begin{pmatrix} R_1 & R_2 & 0 & R_3 & R_4 \\ 0 & 0 & 0 & 0 & 0 \\ 0 & 0 & 0 & 0 & 0 \\ 0 & 0 & 0 & 0 & 0 \\ 0 & 0 & 0 & 0 & 0 \end{pmatrix},$$

where

$$R_1 = \frac{\beta H_0 \eta_3}{\mu + \zeta + \frac{a_3 a_0}{\mu_i}} + \frac{\beta H_0 \eta_2 \zeta}{\left(\mu + \frac{a_3 a_0}{\mu_i}\right) \left(\mu + \zeta + \frac{a_3 a_0}{\mu_i}\right)},$$

$$R_2 = \frac{\beta H_0 \eta_2}{\mu + \frac{a_3 a_0}{\mu_i}}, \quad R_3 = \frac{\beta H_0 \eta_1}{\mu_v}, \quad R_4 = \frac{\beta H_0 \mu_i}{a_0}.$$

$R_1$  is the number of secondary infections caused by one infected hepatocyte in the chronic phase to come up with new infected hepatocytes in the chronic phase.  $R_2$  is the number of secondary infectious hepatocytes in the chronic phase produced by the infected hepatocytes in the cirrhotic phase.  $R_3$  is the number of secondary infected hepatocytes in the chronic phase produced by the external hepatitis B virus.  $R_4$  is the number of secondary infected hepatocytes in the chronic phase produced by the cancer cells.

Therefore, the basic reproduction ratio which is the spectral radius of the next generation matrix,  $FV^{-1}$  is given by:

$$R_0 = \frac{\beta H_0 \eta_3}{\left(\mu + \zeta + \frac{a_3 a_0}{\mu_i}\right)} + \frac{\beta H_0 \eta_2 \zeta}{\left(\mu + \frac{a_3 a_0}{\mu_i}\right) \left(\mu + \zeta + \frac{a_3 a_0}{\mu_i}\right)}.$$

In the reproduction number, the first term represents the number of secondary infections caused by the infected hepatocytes in the chronic phase while the second term represents the number of secondary infections caused by the infected hepatocytes in the cirrhotic phase.

### C. Equilibrium points

We set the right hand side of equations (21) – (26) to zero, so that

$$H^* = \frac{\pi}{\beta(C^* + \eta_3 I_{cr}^* + \eta_2 I_{ci}^* + \eta_1 H_B^{e*}) + \mu}, \quad (29)$$

$$H_B^{e*} = \frac{\delta_r N_1 I_{cr}^* H_B^{i2*}}{(H_B^{i2*} + (N_1 I_{cr}^*)^2) \mu_v} + \frac{\delta_i N_2 I_{ci}^* H_B^{i2*}}{(H_B^{i2*} + (N_2 I_{ci}^*)^2) \mu_v}. \quad (30)$$

From equation (22), we have (see Appendix):

$$I_{cr}^{*5} d_5 + I_{cr}^{*4} d_4 + I_{cr}^{*3} d_3 + I_{cr}^{*2} d_2 + I_{cr}^* d_1 + d_0 = 0. \quad (31)$$

From equation (23), we have (see Appendix):

$$I_{ci}^{*3} b_3 + I_{ci}^{*2} b_2 + I_{ci}^* b_1 + b_0 = 0. \quad (32)$$

From equation (24), we have

$$H_B^{i*} \left( \alpha \left( 1 - \frac{H_B^{i2*}}{H_B^{i2*} + (N_1 I_{cr}^*)^2} \right) + \alpha_1 \left( 1 - \frac{H_B^{i2*}}{H_B^{i2*} + (N_2 I_{ci}^*)^2} \right) - \mu_v - \frac{N_1 \delta_r I_{cr}^* H_B^{i*}}{H_B^{i2*} + (N_1 I_{cr}^*)^2} - \frac{N_2 \delta_i I_{ci}^* H_B^{i*}}{H_B^{i2*} + (N_2 I_{ci}^*)^2} \right) = 0, \quad (33)$$

and the solutions are  $H_B^{i*} = 0$  or the big bracket = 0.

For  $H_B^{i*} = 0$ , our system relates to an HBV-free equilibrium. Once the solutions of  $I_{cr}^*$  and  $I_{ci}^*$  are substituted in non-zero equilibrium point of  $H_B^{i*}$ , the result is an implicit function whose solutions can only be established numerically.

From equation (26), we have

$$C^* \left( \left( \pi_c + (\phi_1 I_{cr}^* + \phi_2 I_{ci}^*) \left( \frac{H_B^{e*}}{H_B^{e*} + c} \right) \right) (C^*)^{-\frac{1}{4}} \times \left( 1 - \left( \frac{C^*}{C_0} \right)^{\frac{1}{4}} \right) - \xi_3 \right) = 0, \quad (34)$$

and the solutions are  $C^* = 0$  or the big bracket = 0.

Note that  $C^* = 0$  corresponds to a cancer free environment. For equation (34), once the solutions of  $I_{cr}^*$ ,  $I_{ci}^*$ ,  $H_B^{e*}$  are in terms of  $C^*$ , their substitution into the non-zero equilibrium point result in an implicit function whose solutions can be established numerically.

1) *Disease free equilibrium:*

$$E_0 = \left( \frac{\pi}{\mu}, 0, 0, 0, 0, 0 \right).$$

2) *Cancer free equilibrium:*

$$E_1 = (H^*, I_{cr}^*, I_{ci}^*, H_B^{i*}, H_B^{e*}, 0).$$

3) *Endemic/cancer-persistence equilibrium:*

$$E_2 = (H^*, I_{cr}^*, I_{ci}^*, H_B^{i*}, H_B^{e*}, C^*),$$

where the expressions of  $H^*$ ,  $I_{cr}^*$ ,  $I_{ci}^*$ ,  $H_B^{i*}$ ,  $H_B^{e*}$  and  $C^*$  are given in equations (29) – (34). For  $E_1$  and  $E_2$  due to mathematical intractability we are unable to explicitly express the endemic states in terms of the model parameters. We shall explore them numerically.

**D. Stability analysis of the equilibrium points**

We shall analyze the stability of  $E_0$  and  $E_2$ . We deliberately leave out  $E_1$  because its analysis is the same as  $E_2$ .

1) *Stability analysis of the disease free case:* According to [29] the stability of the disease free equilibrium point is determined by the stability of the matrix  $F - V$  given by:

$$F - V = \begin{pmatrix} y_0 & \beta H_0 \eta_3 & 0 & \beta H_0 \eta_1 & \beta H_0 \\ \zeta & y_1 & 0 & 0 & 0 \\ 0 & 0 & -(\mu_v + \alpha + \alpha_1) & 0 & 0 \\ 0 & 0 & 0 & -\mu_v & 0 \\ 0 & 0 & 0 & 0 & -\frac{a_0}{\mu_i} \end{pmatrix},$$

where

$$y_0 = \beta H_0 \eta_3 - \left( \mu + \zeta + \frac{a_3 a_0}{\mu_i} \right),$$

$$y_1 = -\left( \mu + \frac{a_3 a_0}{\mu_i} \right).$$

The eigenvalues of  $F - V$  are determined by solving the equation  $|(F - V) - \lambda I| = 0$ , which gives five eigenvalues:

$$\lambda_1 = -\frac{a_0}{\mu_i}, \quad \lambda_2 = -\mu_v, \quad \lambda_3 = -(\mu_v + \alpha + \alpha_1),$$

$$\lambda_{4,5} = \frac{1}{2} \left( -(y_0 + y_1) \pm \sqrt{(y_0 + y_1)^2 + 2y_0 y_1 + 4y_0 y_1 (1 - R_0)} \right).$$

From our eigenvalues:  $\lambda_1, \lambda_2, \lambda_3$  are obviously negative or have negative real parts, and  $\lambda_{4,5}$  is negative or has negative real parts provided  $R_0 < 1$ . Therefore subject to these conditions the disease free equilibrium point is stable.

2) *Stability analysis of the endemic equilibrium point(s):* The stability of the endemic equilibrium point(s)  $E_2$  depends on the stability of the Jacobian matrix ( $J$ ) of the system of equations (21) – (25) given by:

$$J = \begin{pmatrix} -(\lambda^* + \mu) & \beta \eta_3 H^* & \beta \eta_2 H^* & 0 & \beta \eta_1 H^* & \beta H^* \\ \lambda^* & k_1 & k_2 & k_3 & 0 & k_4 \\ 0 & \zeta + k_{18} & k_5 & k_6 & 0 & k_7 \\ 0 & k_8 & k_9 & k_{10} & 0 & 0 \\ 0 & k_{11} & k_{12} & k_{13} & -\mu_v & 0 \\ 0 & k_{14} & k_{15} & 0 & k_{16} & k_{17} \end{pmatrix}$$

The expressions  $k_1$  to  $k_{18}$  are given in the Appendix.

**Theorem 1** ([30]). *Let  $M$  be of size  $n \times n$  with real entries  $M_{ij}$ . If the diagonal elements of that matrix satisfy  $m_{ij} < -r_i$  where  $r_i = \sum_{j=1, j \neq i}^n |m_{ij}|$  for  $i, j = 1 \dots n$ , then the eigenvalues of  $M$  are negative or have negative real parts .*

Applying the Gershgorin Circle Theorem in Theorem 1 to our matrix  $J$  of size  $6 \times 6$  we get the following inequalities:

$$\frac{\beta \eta_3 H^* + \beta \eta_2 H^* + \beta \eta_1 H^* + \beta H^*}{\lambda^* + \mu} < 1,$$

$$\frac{\lambda^* + k_2 + k_3 + k_4}{k_1} < 1,$$

$$\frac{\zeta + k_{18} + k_6 + k_7}{k_5} < 1, \quad \frac{k_8 + k_9}{k_{10}} < 1,$$

$$\frac{k_{11} + k_{12} + k_{13}}{\mu_v} < 1, \quad \frac{k_{14} + k_{15} + k_{16}}{k_{17}} < 1. \quad (35)$$

Hence, the equilibrium point(s)  $E_2$  is locally stable only when the conditions in (35) are satisfied.

**IV. PARAMETER ESTIMATION, IMMUNOTHERAPY AND NUMERICAL SIMULATIONS**

In this section, we present numerical simulation results of the model. We shall only focus on the cancer persistent equilibrium simulation results since we are applying immunotherapy against the cancer cells. The results on the cancer free endemic equilibrium are not of interest to this study and hence, we do not discuss them here. Firstly, we shall carry out parameter estimation using the FME algorithm. Secondly, we shall introduce immunotherapy in the

form of pharmacokinetic dynamics of Nivolumab as a representative immunotherapeutic drug, Thirdly, we shall use the pharmacokinetic parameters of Nivolumab as a monoclonal antibody to demonstrate drug effects in the sub-therapeutic, therapeutic and toxic regions of the drug. Lastly, we shall incorporate the effects of missing doses on the therapeutic window of the drug.

A. Parameter estimation

We estimate parameter values in Table 2 for our model by using parameters from published literature, assumed values and apply inverse modelling [31] to find reasonable values for our parameters in our model using the Flexible Modelling Environment (FME). FME is a modelling package designed to confront a mathematical model with data and uses algorithms for sensitivity analysis and Monte Carlo analysis, parameter identifiability and model fitting [31]. Assigning the known parameter values and solving the model numerically produced reasonable qualitative features of the healthy hepatocytes, both the infected hepatocytes, the internal and external virus and also the cancer cells as shown in Figure 2 which represents a cancer persistent equilibrium.

The FME procedure produced weighted residuals plots in Figure 3, which suggest that the relationship between the state variables in the plots is linear. Sensitivity analysis plots on  $H_B^i$ ,  $I_{cr}$ ,  $I_{ci}$ ,  $H_B^e$  and  $C$  are shown in Figures 4a, 4b, 4c, 4d and 4e. From Figure 4a, based on the summary statistics in Table 3, the parameters  $\phi_1$ ,  $\beta$ ,  $\mu$ ,  $\phi_2$ ,  $\mu_8$  and  $\mu_a$  have the least effects on the output variables on internal HBV and  $\delta_r$ ,  $c$ ,  $\eta_3$ ,  $\alpha_1$ ,  $k_r$ ,  $k_i$ ,  $\nu_i$ ,  $ca$  have a consistent positive effect on the internal HBV and  $\pi$ ,  $\pi_c$ ,  $C_0$ ,  $\eta_1$ ,  $\alpha_3$ ,  $\delta_i$ ,  $k_c$ ,  $\mu_i$ ,  $\pi_4$ ,  $\pi_i$ ,  $\mu_4$ ,  $\gamma$ ,  $\pi_a$ ,  $\nu_r$ ,  $ci$  and  $\pi_8$  have a consistent negative effect on the internal HBV. A similar analysis can be done for figures 4b, 4c, 4d and 4e with their corresponding sensitivity summary statistics values. Picking the best-fit from Figures 5a – 5e, we obtain the best-fit parameter values shown in Table 2. We shall use the best-fit parameters for our simulations.

B. Numerical simulations

We use the parameter values obtained from the FME algorithm to the model with immunotherapy to observe the trends of the cancer cells, the healthy hepatocytes, the infected hepatocytes ( $I_{cr}$  and  $I_{ci}$ ) and the internal and external hepatitis B virus.

1) *Pharmacokinetics of Nivolumab:* After taking a drug, concentration levels peak quickly to a maximum concentration then drop slowly to a minimum

Parameters	Value	References
$C_{max}$	240 mg/kg	[8, 34]
$C_{min}$	0.1	This work
$T_{max}$	1 to 4 hours	[8, 34]
$k$	0.7783	Calculated
$\tau$	14	[8, 34]

Table 1: Pharmacokinetics parameter values for Nivolumab.

concentration as the drug is eliminated. The highest concentration is called the  $C_{max}$ . The time taken to get to the highest concentration is called the  $T_{max}$ . When a drug is taken routinely as treatment, the lowest concentration just before the next dose is called the  $C_{min}$  [32]. We define the efficacy function for the treatment using Nivolumab as an intervention drug as:

$$\epsilon_{Niv}(t) = \frac{C(t)}{IC_{50} + C(t)}, \tag{36}$$

where  $C(t)$  is the drug concentration in the cancer cells,  $IC_{50}$  is the intracellular saturation concentration necessary to inhibit the cancer cells replication by 50 percent. We adopt the concentration drug introduced in [33] defined as:

$$C(t) = \begin{cases} C_{min} + \frac{(C_{max} - C_{min})(1 - \exp(-t))}{1 - \exp(-T_{max})}, & t \in [t_i, T_{max}], \\ C_{max} \exp\left(-\frac{\ln(C_{max}) - \ln(C_{min})}{\tau - T_{max}}(t - T_{max})\right), & t \in [T_{max}, \tau + t_i], \end{cases}$$

where the parameter  $\tau$  is the dosage interval,  $t_i$  is the starting time of the  $i$ -th dose. Table for parameter values for pharmacokinetics of Nivolumab is given in Table 1. As earlier stated in the introduction, we use monoclonal antibody type of treatment for HCC that targets the growth signal in cancer cells hence we build up the treatment function in the cancer cells dynamics and this modifies equation (26) to become:

$$\frac{dC}{dt} = (1 - \epsilon_{Niv}(t)) \left(1 - \left(\frac{C}{C_0}\right)^{\frac{1}{4}}\right) \times \left(\pi_c + (\phi_1 I_{cr} + \phi_2 I_{ci}) \left(\frac{H_b^e}{H_B^e + c}\right)\right) C^{\frac{3}{4}} - \xi_3 C.$$

2) *Concentration regions of Nivolumab:* When a drug is administered, various drug concentrations may be categorised into three main regions, namely: the sub-therapeutic region, the therapeutic region and the toxic region. The therapeutic region is a range of doses

between minimum effective concentration (MEC) and the minimum toxic concentration (MTC). The sub-therapeutic region is a range of doses between  $C_{min}$  and the MEC and the toxic region are doses above the MTC. Drug levels are required to be between MEC and MTC for desired efficacy. Drug levels that cross MTC elicit toxic effects and drug levels that are unable to surpass MEC cause a sub-therapeutic effect [32]. Figure 6a is an example of Nivolumab concentration in the sub-therapeutic region and the therapeutic region over 2 doses. Since the minimum and maximum levels of toxicity concentration is not clear, we carry out an exhaustive analysis of all the cases around the definition of toxicity and three scenarios to the definition arise. Scenario 1 the minimum and maximum concentration of a drug is always above the MTC, Scenario 2 the minimum concentration is in the therapeutic region while the maximum concentration is above the MTC and scenario 3 the minimum concentration is below the MEC while the maximum concentration is above the MTC. Figure 6b illustrates the scenarios of the toxic regions of Nivolumab over two doses. Figure 6c shows the corresponding efficacies of three different regions, sub-therapeutic, therapeutic and the scenarios of toxicity of Nivolumab using the efficacy function in equation (36). In the case of Nivolumab, the MTC is 240mg/kg and the MEC 50mg/kg. The MTC is also called the adverse response threshold (ADT) and the MEC is also called the desired response threshold (DRT).

3) *Simulation results:* We demonstrate the regions where the drug efficacy is sub-therapeutic, therapeutic and toxic in the healthy hepatocytes, the cancer cells, the infected hepatocytes in the chronic phase, the infected hepatocytes in the cirrhotic phase and the internal and external HBV shown in figures 8a – 8f. For the purpose of this study, we focus our results on the trends of the cancer cells as they are the indicators of HCC progression. Trends of the healthy hepatocytes, the infected cells and the viruses are also presented. We shall call the sub-therapeutic region, region I, the therapeutic region, region II and the three toxic regions; region  $III_1$ ,  $III_2$  and  $III_3$ .

Figures 8a – 8f, represent the Nivolumab effects in the sub-therapeutic region I, the therapeutic region II and the toxic region  $III_1$ . Increasing Nivolumab in region I reduces the population of cancer cells. Region II represents the desired effects of Nivolumab to reducing the cancer cells. Increasing concentration towards the MTC gives better results in reducing the cancer cells. Increasing concentration to region  $III_1$

reduces the cancer cells but this is associated with toxic effects. In Figure 8b, we observe that there is a slight increase in the healthy hepatocyte population when the concentration of a drug is increased. In Figures 8c – 8f, we observe that the infectious populations are decreasing from effects ranging from sub-therapeutic to therapeutic to toxic.

Figures 9a – 9d represent the Nivolumab effects in the sub-therapeutic region I, the therapeutic region II and the toxic regions  $III_2$  and  $III_3$  in the cancer cells and the healthy hepatocytes. We observe a great increase in cancer cells coming from effects from toxic region  $III_3$  followed by toxic region  $III_2$  and corresponding decrease of healthy hepatocytes from effects of toxic region  $III_3$  followed by region  $III_2$ . The counter effect is all of the outcomes from toxic regions  $III_1$ ,  $III_2$  and  $III_3$  lead to toxic effects with terrible results coming from region  $III_1$  followed by region  $III_2$  and then region  $III_3$ . They also lead to an increase in cancer cells population with most effects coming from region  $III_3$  followed by region  $III_2$  and lastly region  $III_1$ . The recovery of healthy hepatocytes is observed from regions ranging from  $III_1$  to  $III_2$  to  $III_3$ .

We also illustrate the effects sub-optimal adherence. We show trends on missing every subsequent dose and every two subsequent doses in the therapeutic window. Figure 7a portrays the concentration of Nivolumab upon missing a single dose and missing two doses. Figure 7b – 7c illustrates the corresponding effects of missing a single dose and two doses on the dynamics of the cancer cells and the healthy hepatocytes respectively. We observe that missing one dose reduces the effectiveness of the drug in the therapeutic window and missing two doses reduces the effectiveness of the drug to the sub-therapeutic window. Further missing one dose has almost similar effects to toxic effects in region  $III_2$  and missing two doses has almost similar effects to toxic effects in region  $III_3$ .

## V. DISCUSSION OF RESULTS AND CONCLUSION

To investigate the pharmacokinetic effects of immunotherapy as an intervention strategy for Hepatocellular carcinoma, our model presented a simplified structure of a complex biological interaction of hepatocytes, immune cells, cytokines, cancer cells and hepatitis B virus. From our model analysis, we proved that the state variables of the model were positive and bounded in a biologically feasible region and obtained the basic reproduction number and identified it was influenced by secondary infections caused by the infected hepatocytes

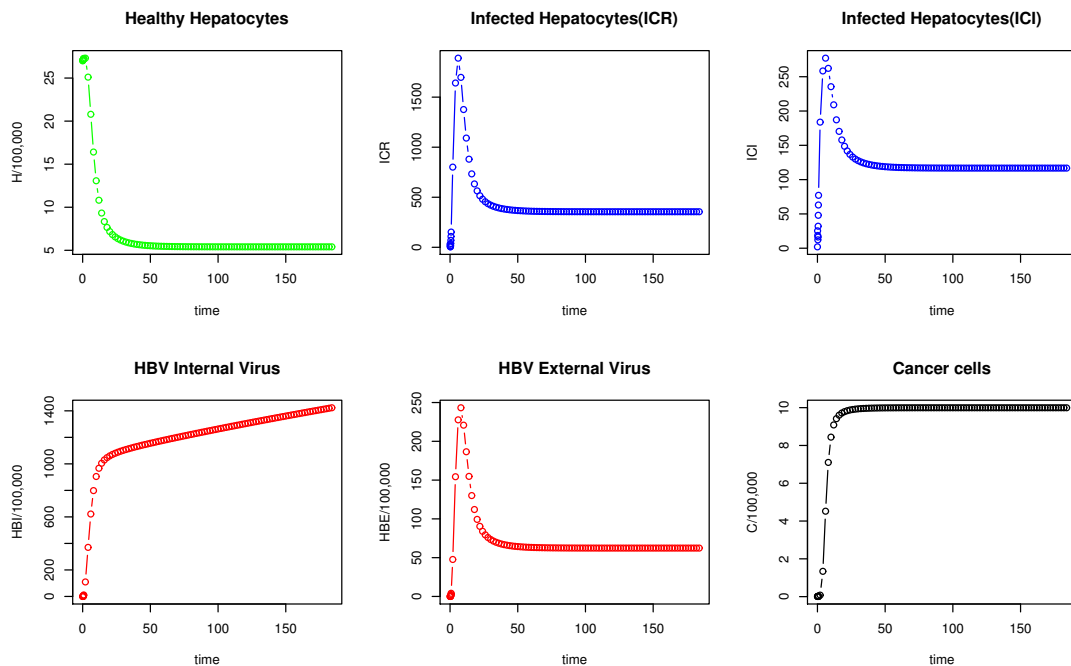


Fig. 2: R plots.

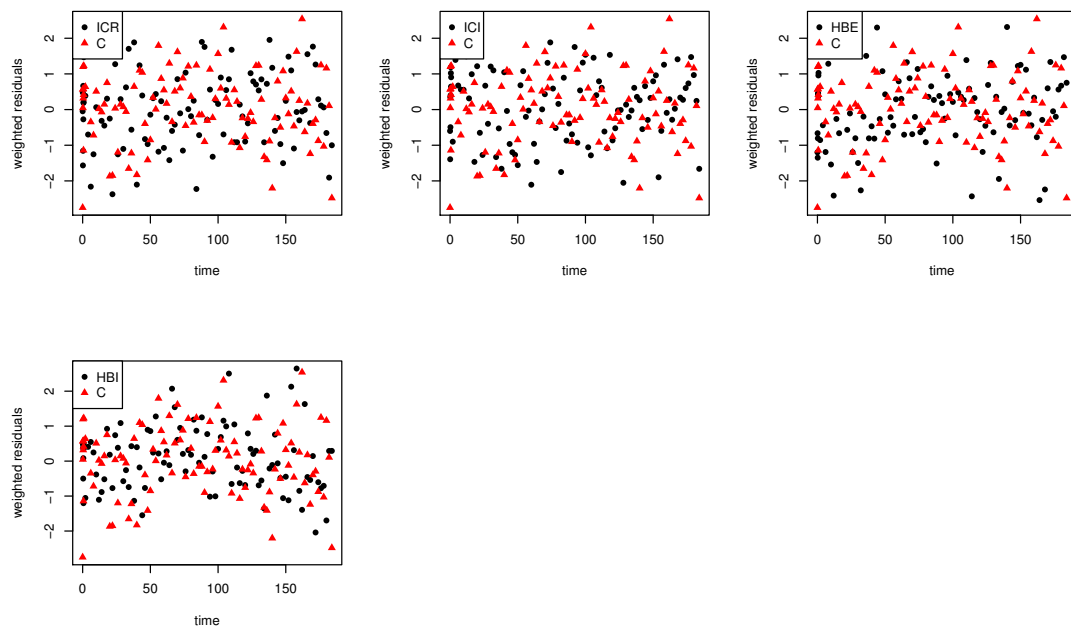
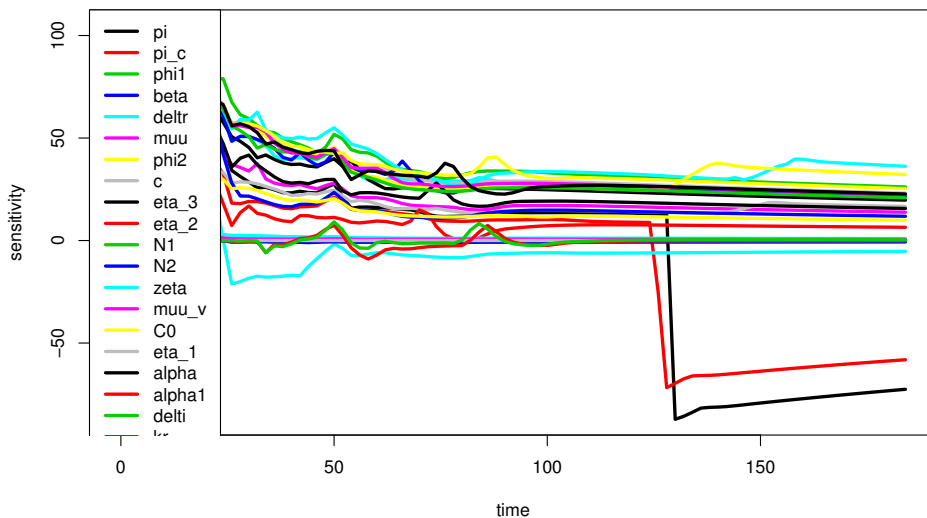


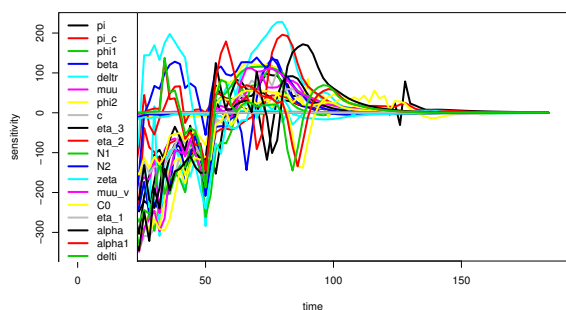
Fig. 3: Residuals of model and pseudodata.

**HBI**



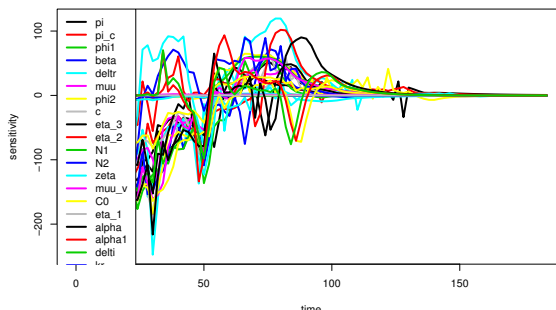
(a) HBI sensitivity functions to parameters.

**ICR**



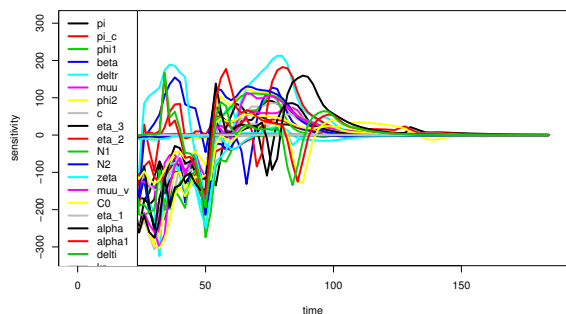
(b) ICR sensitivity functions to parameters.

**ICI**



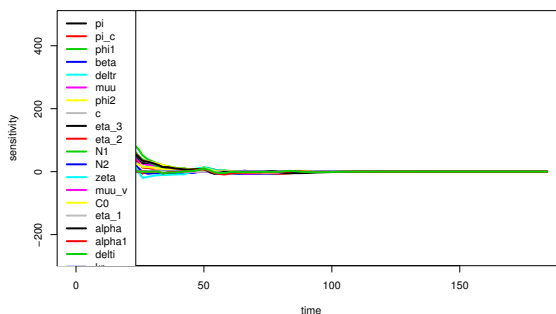
(c) ICI sensitivity functions to parameters.

**HBE**



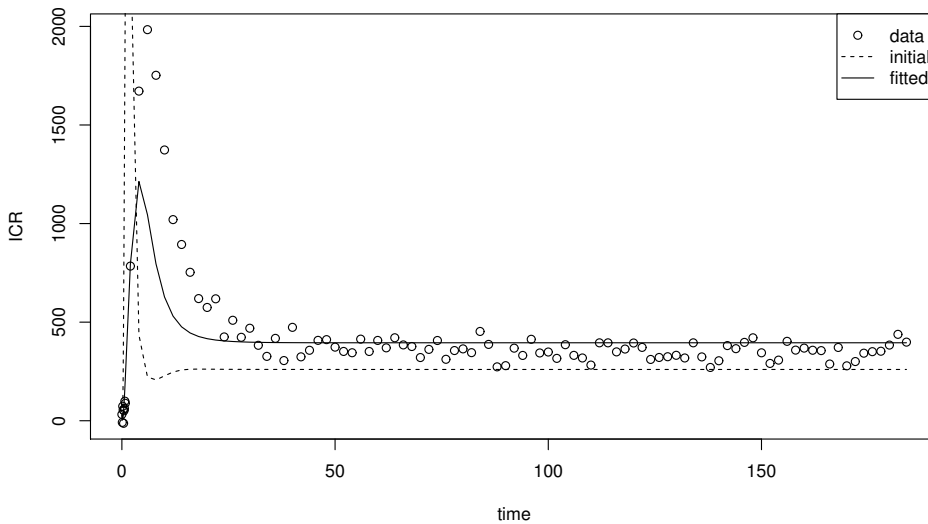
(d) HBE sensitivity functions to parameters.

**C**

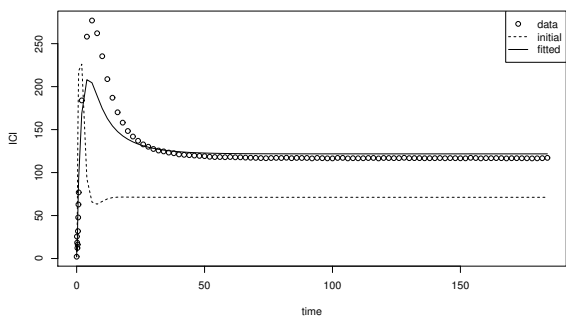


(e) C sensitivity functions to parameters.

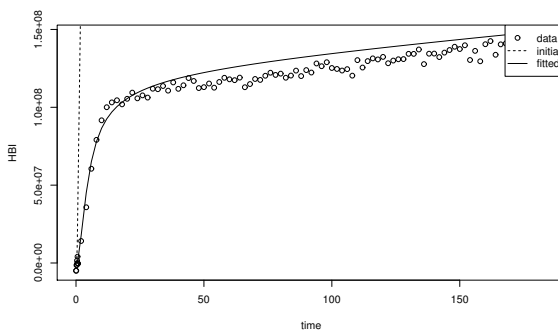
Fig. 4: Sensitivity functions to parameters.



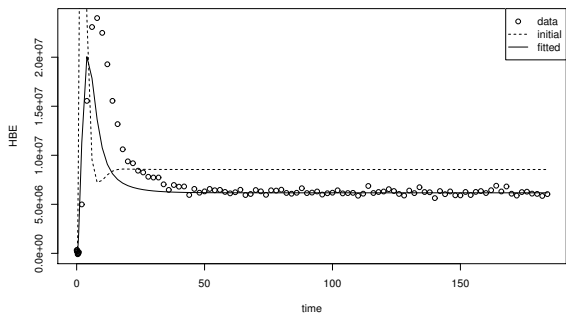
(a) ICR bestfit and initial run.



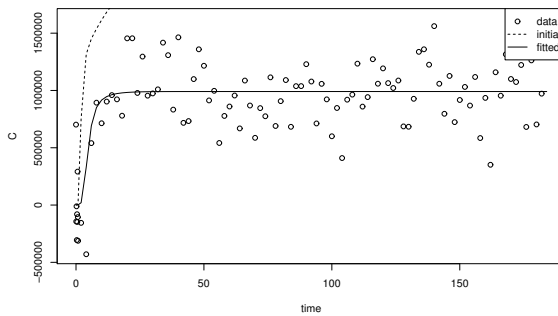
(b) ICI bestfit and initial run.



(c) HBI bestfit and initial run.

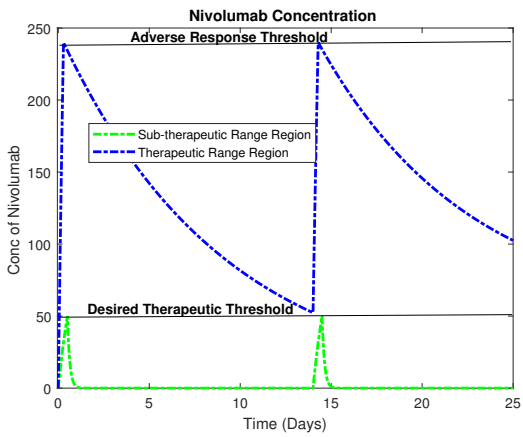


(d) HBE bestfit and initial run.

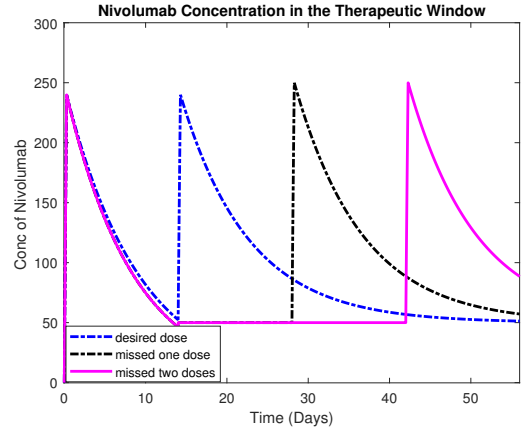


(e) C bestfit and initial run.

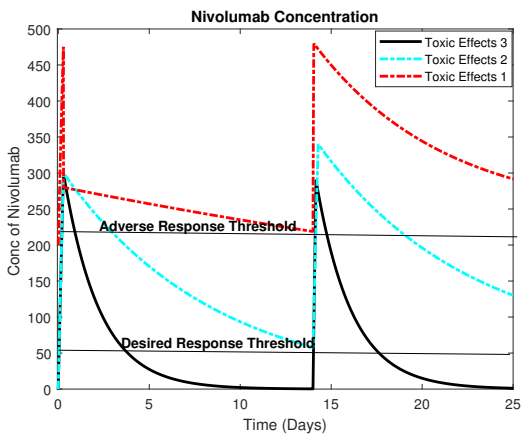
Fig. 5: Bestfit and initial run.



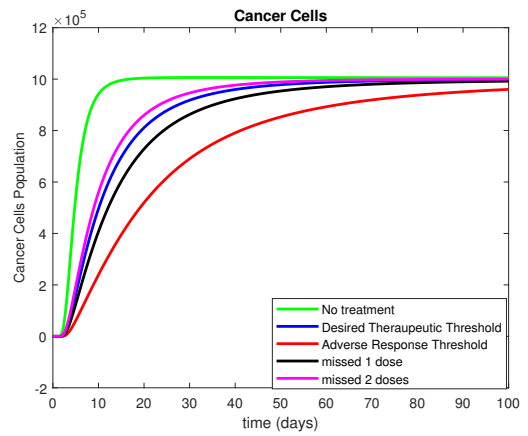
(a)



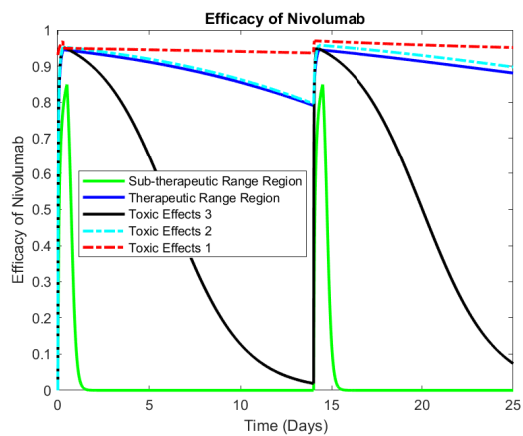
(a) Missing Nivolumab doses.



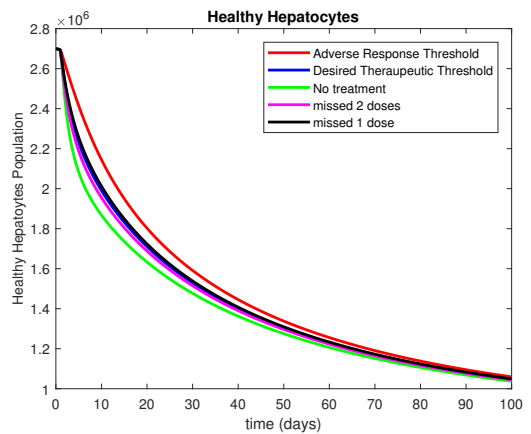
(b)



(b) Cancer cells.



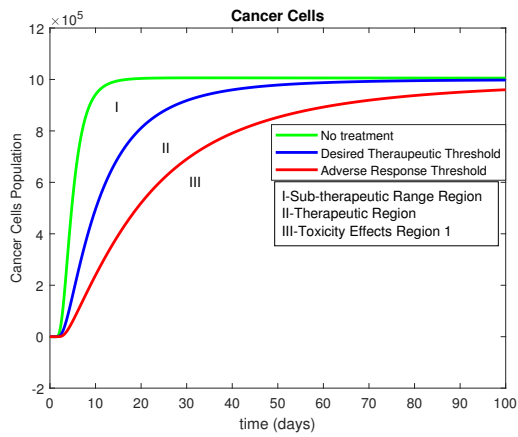
(c)



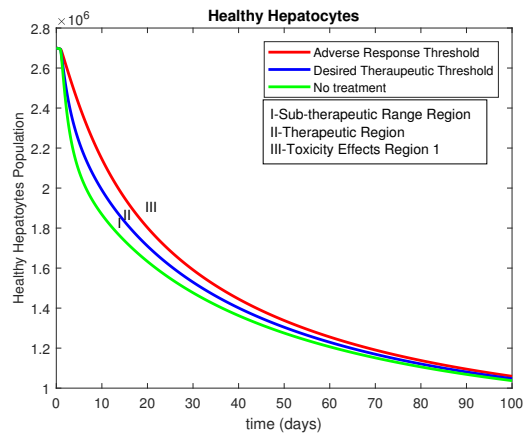
(c) Healthy hepatocytes.

Fig. 6: Nivolumab response graphs and efficacies.

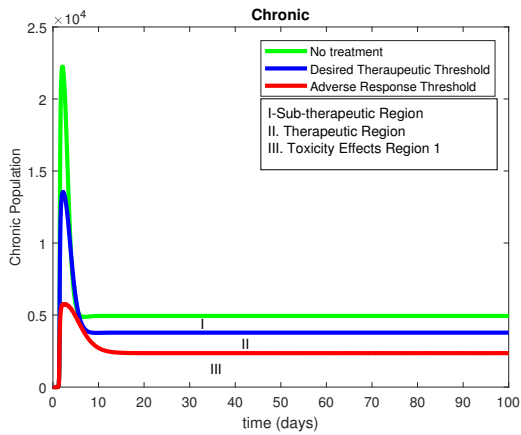
Fig. 7: Concentration of Nivolumab upon missing a single dose and missing two doses.



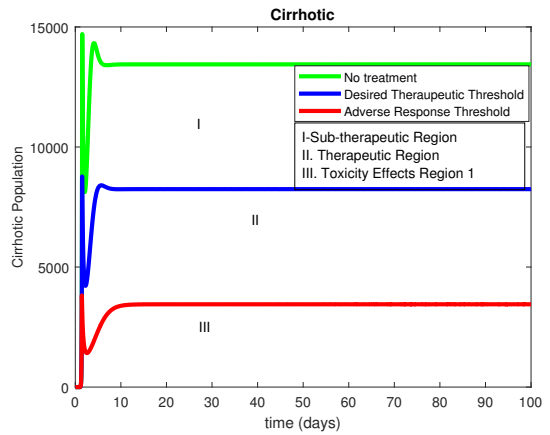
(a) Cancer cells.



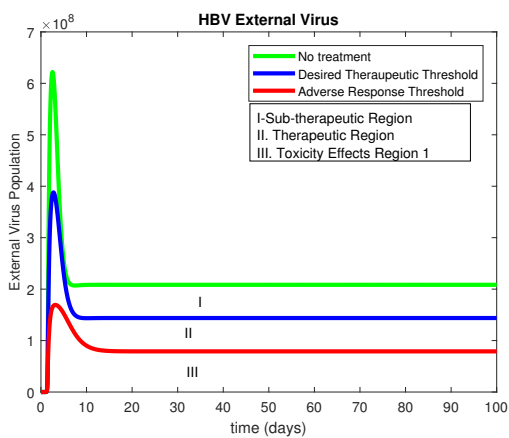
(b) Healthy hepatocytes.



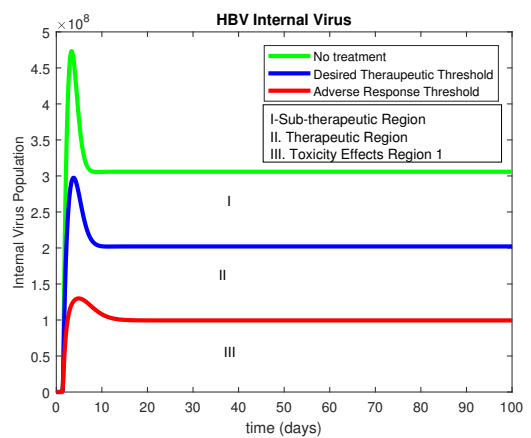
(c)  $I_{Cr}$  hepatocytes.



(d)  $I_{Cri}$  hepatocytes.



(e) HBV external.



(f) HBV internal.

Fig. 8: Nivolumab effects in the sub-therapeutic region I, the therapeutic region II and the toxic region III<sub>1</sub>.

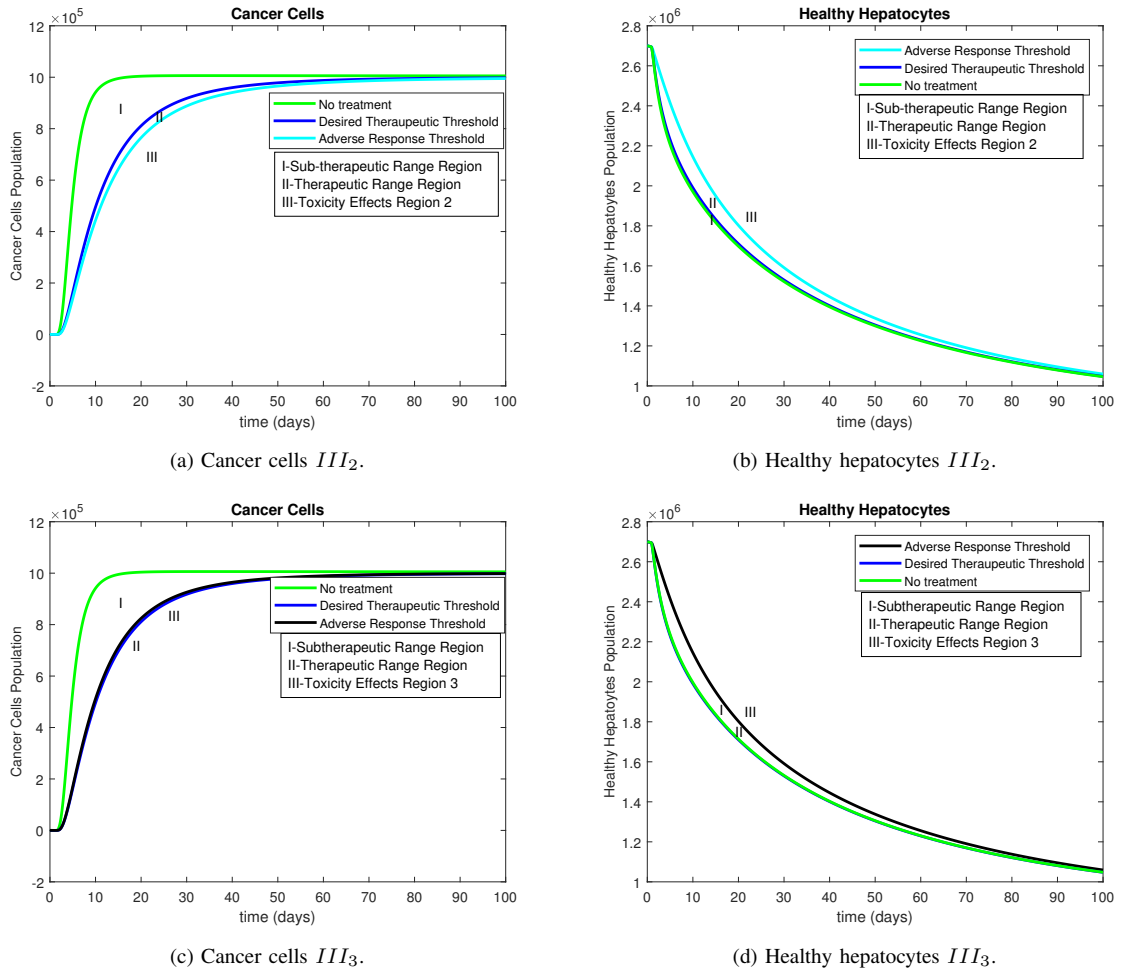


Fig. 9: Nivolumab effects in the sub-therapeutic region I, the therapeutic region II and the toxic regions  $III_2$  and  $III_3$ .

from the chronic phase, infected hepatocytes from the cirrhotic phase and the cancer cells. The mathematical analysis showed the existence of three equilibrium points namely: the disease free equilibrium point which implies there is no cancer, the cancer free equilibrium point which implies one is in the chronic stage and the cancer persistence equilibrium point which implies one has cancer. The threshold conditions for local stability for the equilibrium points were established using the Watmough and Van den Driessche’s method [29] for local stability and also the Gersgorin Circle Theorem [30].

Some parameter values were assumed and some obtained from literature. We fitted our model to experimental data using inverse modelling to find reasonable values for our parameters. Since within host parameter

values are not directly measurable and costly, their estimation was obtained from the flexible modelling environment (FME) algorithm which amounts to determining the unknown physical parameters by fitting the observed histories [31]. Even though the prediction from these estimates remain theoretical, they are qualitatively robust and trustable. We used estimates from this algorithm for our model to carry out our simulations.

From our results, we believe that predictions of our model with the inclusion of immune cells and cytokine responses involved give a more realistic picture of the hepatitis B infection in hepatocellular carcinoma and we argue that studies that have modeled hepatocellular carcinoma without the inclusion of the immune cells and cytokines may have lost valuable information on

Parameters	Known Values	FME Values
$\pi$	18090	5.157363e+04
$\beta$	0.6079e-08	3.784784e-09
$\zeta$	20.9	3.545362e+01
$\alpha$	30	4.373477e+03
$\delta_r$	2.9043	5.829264e+00
$\delta_i$	5.7043	9.682311e+00
$N_1$	2500	4.373477e+03
$N_2$	2400	2.216137e+03
$\mu$	0.0067	1.525115e-02
$\mu_v$	0.67	1.331681e+00
$\pi_c$	0.003	5.430826e-03
$\alpha_1$	25	2.216137e+03
$\phi_1$	0.02	4.689978e-02
$\phi_2$	0.05	9.313445e-02
$\eta_1$	0.5	1.019040e+00
$\eta_2$	0.7	1.398464e+00
$\eta_3$	0.9	1.761110e+00
$c$	50000	7.748552e+05
$C_0$	$10^6$	9.915831e+05
$\pi_4$	0.004	8.000000e-03
$\pi_i$	0.001	2.000000e-03
$c_i$	200	3.751750e+02
$k_r$	100	2.083608e+02
$k_i$	150	4.290720e+02
$k_c$	200	4.187280e+02
$\mu_i$	0.45	9.000455e-01
$\mu_4$	0.002	4.000000e-03
$\pi_8$	0.002	2.806285e-03
$\gamma$	0.033	6.815085e-02
$\pi_4$	0.044	8.000000e-03
$\mu_8$	0.02	3.997595e-02
$c_a$	300	6.112113e+02
$\nu_r$	100	1.939661e+02
$\nu_i$	150	3.422596e+02
$\mu_a$	9.68	1.934606e+01

Table 2: Table for known parameter values vs FME parameter values.

model predictions. Further, mathematical models that incorporate pharmacokinetic effects to treatment have a potential of capturing the true desirable effects of a drug and also expose trends that reflect toxic effects of the drug as well as the sub-therapeutic effects of the drug. Thus, our model predictions give a realistic picture of modeling the treatment of hepatocellular carcinoma

Simulation results showed that immunotherapy has the potential to delay the growth of cancer cells when the drug concentrations are increased. However because some drug concentrations fall within the toxic regions, the benefits for such drugs concentrations will have corresponding adverse effects. Hence, care should be drawn to the effects of the immunotherapy concentrations within the therapeutic region. Concentrations in the sub-therapeutic region showed to have slight

benefits which are almost close to no treatment. Our results suggests toxicity of the three different categories depicted in regions  $III_1$ ,  $III_2$  and  $III_3$ . The greatest toxicity is presumed to come from region  $III_1$  followed by region  $III_2$  and then region  $III_3$ . Some studies that investigated toxicity [35, 36] only tackled its effects associated to region  $III_1$ . Our model has therefore revealed some of the cases that can arise from toxicity effects that have been demonstrated in scenarios  $III_2$  and  $III_3$ . An interesting observation is that toxicity of region  $III_2$  replicate effects of a drug in the therapeutic region II whilst toxicity effects of region  $III_3$  show effects of a drug in the sub-therapeutic region I. Region  $III_2$  would represent a drug whose effects on cancer cells are similar to those from the therapeutic window and yet having side effects. Region  $III_3$  would represent a drug whose effects on cancer cells are similar to those from the sub-therapeutic region and also having side effects. Missing doses either reduced the effectiveness of the drug to sub-therapeutic window or in the therapeutic window. It was also interesting to observe that concentration in toxic region  $III_2$  had effects similar to missing one dose and toxic concentration in region  $III_3$  had similar effects to missing two doses. Hence it is not only toxic effects of a drug that are not good, even missing of doses in the therapeutic window can achieve similar devastating effects as toxicity the difference being missing doses in the therapeutic window will not give toxic effects but overall all lead to inefficient suppression of cancer cells.

In conclusion, modeling of treatment should be done using realistic pharmacokinetics of a drug and we would be able to show the concentration effects of a drug within the different regions. In particular, our study revealed that it is not only how far the levels of cancer markers are reduced but the concentration should also be associated to the appropriate desirable therapeutic concentrations in the therapeutic window region as well as the perfect adherence of the drug. Any deviations from these may lead to undesirable effects.

#### ACKNOWLEDGEMENTS

This work was carried out with the aid of a grant in the UNESCO-TWAS programme, “Seed Grant for African Principal Investigators” financed by the German Federal Ministry of Education and Research (BMBF). The views expressed herein do not necessarily represent those of UNESCO-TWAS or BMBF.

	Value	Scale	$L_1$	$L_2$	Mean	Min	Max	N
$\pi$	1.8e+04	1.8e+04	24.500	3.3006	-0.458	-2.2e+02	291.943	202
$\pi_c$	3.0e-03	3.0e-03	0.039	0.0094	-0.011	-1.0e+00	1.422	202
$\phi_1$	2.0e-02	2.0e-02	0.307	0.0633	0.164	-4.3e+00	10.394	202
$\beta$	6.1e-09	6.1e-09	0.136	0.0319	0.135	-6.8e-03	4.685	202
$\delta_r$	2.9e+00	2.9e+00	17.477	1.9779	14.888	-1.8e+02	93.461	202
$\mu_u$	6.7e-03	6.7e-03	0.109	0.0147	0.073	-1.8e+00	0.376	202
$\phi_2$	5.0e-02	5.0e-02	0.670	0.1506	0.461	-8.6e+00	26.142	202
$c$	5.0e+04	5.0e+04	18.895	2.1313	16.114	-1.8e+02	129.451	202
$\eta_3$	9.0e-01	9.0e-01	16.107	1.8027	13.642	-1.6e+02	83.891	202
$\eta_2$	7.0e-01	7.0e-01	18.878	2.4830	-1.556	-1.6e+02	205.874	202
$N_1$	2.5e+03	2.5e+03	24.172	3.4187	19.936	-2.5e+02	475.372	202
$N_2$	2.4e+03	2.4e+03	17.533	1.9794	14.875	-1.8e+02	93.312	202
$\zeta$	2.1e+01	2.1e+01	25.357	3.4350	21.643	-2.0e+02	481.590	202
$\mu_v$	6.7e-01	6.7e-01	11.506	1.3128	9.451	-1.2e+02	62.220	202
$C_0$	1.0e+06	1.0e+06	19.966	2.1835	16.978	-1.8e+02	130.403	202
$\eta_1$	5.0e-01	5.0e-01	10.121	1.1091	8.696	-9.2e+01	64.728	202
$\alpha$	3.0e+01	3.0e+01	17.272	3.0882	12.707	-2.7e+02	474.166	202
$\alpha_1$	2.5e+01	2.5e+01	7.508	1.1972	6.694	-6.9e+00	127.170	202
$\delta_i$	5.7e+00	5.7e+00	17.416	1.9663	14.244	-1.8e+02	93.028	202
$k_r$	1.0e+02	1.0e+02	13.957	2.1701	7.390	-2.6e+02	90.799	202
$k_i$	1.5e+02	1.5e+02	10.942	2.7772	1.519	-1.5e+02	478.065	202
$k_c$	2.0e+02	2.0e+02	18.523	2.0828	15.674	-1.7e+02	129.945	202
$\mu_i$	4.5e-01	4.5e-01	8.276	0.9372	6.811	-8.3e+01	58.258	202
$\pi_4$	4.0e-03	4.0e-03	0.074	0.0084	0.063	-7.3e-01	0.518	202
$\pi_i$	1.0e-03	1.0e-03	0.021	0.0023	0.018	-1.8e-01	0.093	202
$\mu_4$	2.0e-03	2.0e-03	0.038	0.0043	0.033	-3.7e-01	0.259	202
$\pi_8$	2.0e-03	2.0e-03	0.202	0.0229	-0.191	-2.0e+00	0.182	202
$\gamma$	3.3e-02	3.3e-02	0.605	0.0979	-0.265	-6.7e+00	15.340	202
$\pi_a$	4.4e-02	4.4e-02	0.796	0.0909	0.655	-8.1e+00	5.697	202
$\mu_8$	2.0e-02	2.0e-02	0.485	0.0736	0.332	-4.4e+00	10.960	202
$v_r$	1.0e+02	1.0e+02	19.836	2.2009	17.338	-1.8e+02	129.455	202
$\mu_a$	9.7e+00	9.7e+00	0.000	0.0000	0.000	0.0e+00	0.000	202
$c_i$	2.0e+02	2.0e+02	18.493	2.0979	15.583	-1.8e+02	129.472	202
$v_i$	1.5e+02	1.5e+02	1.131	0.1580	-0.465	-9.0e+00	8.118	202
$c_a$	3.0e+02	3.0e+02	0.895	0.1298	-0.045	-6.1e+00	9.616	202

Table 3: Summary of sensitivity statistics values.

REFERENCES

[1] H. B. El-Serag, K. L. Rudolph, Hepatocellular Carcinoma: Epidemiology and Molecular Carcinogenesis, *Gastroenterology*, 132:2557–2576, 2007.

[2] H. B. El-Serag, Epidemiology of Viral Hepatitis and Hepatocellular Carcinoma, *Gastroenterology*, 142:1264–1273, 2012.

[3] H. B. El-Serag, A. C. Mason, Rising Incidence of Hepatocellular Carcinoma in the United States, *The New England Journal of Medicine*, 340:745–750, 1999.

[4] P. Matar, L. Alaniz, V. Rozados, J. B. Aquino, M. Malvicini, C. Atorrasagasti, M. Gidekel, M. Silva, O. G. Scharovsky, G. Mazzolini, Immunotherapy for liver tumors: present status and future prospects, *Journal of Biomedical Science*, 16:30, 2009.

[5] J. Bruix, M. Sherman, Management of hepatocellular carcinoma, *Hepatology*, 42:1208–1236, 2005.

[6] K. Palucka, J. Banchereau, Cancer immunotherapy via dendritic cells, *Nature Reviews Cancer*, 12:265–277, 2012.

[7] S. Rosenberg, J. Yang, N. Restifo, Cancer immunotherapy: moving beyond current vaccines, *Nature Medicine*, 10:909–915, 2004.

[8] F. Finkelmeier, O. Waidmann, J. Trojan, Nivolumab for the treatment of hepatocellular carcinoma, *Expert Review of Anticancer Therapy*, 18:1169–1175, 2018.

[9] New Anti-Cancer Therapy – Immune Checkpoint Inhibitors, Medsafe: New Zealand Medicines and Medical Devices Safety Authority, 2017, [18/12/2024].

[10] G. D. Mazzolini, M. Malvicini, Immunostimulatory monoclonal antibodies for hepatocellular carcinoma therapy. Trends and perspectives, *Medicina (Buenos Aires)*, 78:29–32, 2018.

[11] D. Pardoll, Cancer and the Immune System: Basic Concepts and Targets for Intervention, *Seminars in Oncology*, 42:523–538, 2015.

[12] J. B. Swann, M. J. Smyth, Immune surveillance of tumors, *The Journal of Clinical Investigation*, 117:1137–1146, 2007.

[13] M. L. Disis, Immune Regulation of Cancer, *Journal of Clinical Oncology*, 28:4531–4538, 2010.

[14] P. J. Delves, S. J. Martin, D. R. Burton, I. M. Roitt, *Roitt’s Essential Immunology*, John Wiley and Sons, 2017.

[15] V. B. Matthews, G. C. Yeoh, Liver Stem Cells, *IUBMB Life*, 57:549–553, 2005.

[16] H. Ledford, Cancer cells can ‘infect’ normal neighbours, *Nature News*, 2014.

[17] E.-C. Shin, P. S. Sung, S.-H. Park, Immune responses and immunopathology in acute and chronic viral hepatitis, *Nature Reviews Immunology*, 16:509–523, 2016.

[18] M. K. Maini, A. J. Gehring, The role of innate immunity in the immunopathology and treatment of HBV infection, *Journal of Hepatology*, 64:S60–S70, 2016.

[19] T. Reiberger, Y. Chen, R. R. Ramjiawan, T. Hato, C. Fan, R. Samuel, S. Roberge, P. Huang, G. Y. Lauwers, A. X. Zhu, N. Bardeesy, R. K. Jain, D. G. Duda, An orthotopic mouse model of hepatocellular carcinoma with underlying liver cirrhosis, *Nature Protocols*, 10:1264–1274, 2015.

[20] J. Gabriellsson, W. J. Jusko, L. Alari, Modeling of dose-response-time data: four examples of estimating the turnover parameters and generating kinetic functions from response profiles, *Biopharmaceutics and Drug Disposition*, 21:41–52, 2000.

[21] A. L. Mescher, *Junqueira's Basic Histology: Text and Atlas*, McGraw Hill, New York, 2018.

[22] Z. Shuai, M. W. Y. Leung, X. He, W. Zhang, G. Yang, P. S. C. Leung, M. E. Gershwin, Adaptive immunity in the liver, *Cellular and Molecular Immunology*, 13:354–368, 2016.

[23] G. B. West, J. H. Brown, B. J. Enquist, A general model for ontogenetic growth, *Nature*, 413:628–631, 2001.

[24] Y. Louzoun, C. Xue, G. B. Lesinski, A. Friedman, A mathematical model for pancreatic cancer growth and treatments, *Journal of Theoretical Biology*, 351:74–82, 2014.

[25] E. Itakura, N. Mizushima, p62 targeting to the autophagosome formation site requires self-oligomerization but not LC3 binding, *Journal of Cell Biology*, 192:17–27, 2011.

[26] S. Friberg, S. Mattson, On the growth rates of human malignant tumors: Implications for medical decision making, *The Journal of Surgical Oncology*, 65:284–297, 1997.

[27] B. F. Zamarron, W.-J. Chen, Dual Roles of Immune Cells and Their Factors in Cancer Development and Progression, *International Journal of Biological Sciences*, 7:651–658, 2011.

[28] T. L. Whiteside, Immune suppression in cancer: Effects on immune cells, mechanisms and future therapeutic intervention, *Seminars in Cancer Biology*, 16:3–15, 2006.

[29] P. van den Driessche, J. Watmough, Reproduction numbers and sub-threshold endemic equilibria for compartmental models of disease transmission, *Mathematical Biosciences*, 180:29–48, 2002.

[30] L. J. S. Allen, *An Introduction to Mathematical Biology*, Pearson, Prentice Hall, 2007.

[31] K. Soetaert, T. Petzoldt, Inverse Modelling, Sensitivity and Monte Carlo Analysis in R Using Package FME, *Journal of Statistical Software*, 33:1–28, 2010.

[32] A. H. Tashjian, E. J. Armstrong, *Principles of Pharmacology: The Pathophysiologic Basis of Drug Therapy*, Lippincott Williams and Wilkins, 2011.

[33] Sutimin, F. Chirove, E. Soewono, N. Nuraini, L. B. Suromo, A model incorporating combined RTIs and PIs therapy during early HIV-1 infection, *Mathematical Biosciences*, 285:102–111, 2017.

[34] D. A. Solimando Bcop, Jr., J. A. Waddell, Nivolumab and Olaparib, *Hospital Pharmacy*, 50:356–366, 2015.

[35] Á. Norton, J. Sathish, S. Webb, L. Aarons, K. Beattie, R. Eljazi, N. Pearson, R. Rajoli, D. Reddyhoff, M. Siccardi, D. Williams, Mathematical Modelling of Chronic Drug Infusion for Toxicity Assessment, *UK Mathematics-in-Medicine NC3Rs Study Group*, 25, 2013.

[36] M. M. Hadjiandreou, G. D. Mitsis, Mathematical Modeling of Tumor Growth, Drug-Resistance, Toxicity, and Optimal Therapy Design, *IEEE Transactions on Biomedical Engineering*, 61:415–425, 2014.

APPENDIX

$$a_0 = \frac{\pi_4 \pi_i}{\mu_4},$$

$$a_1 = \frac{\pi_8 \pi_a}{\mu_8},$$

$$a_3 = \frac{\gamma \pi_8}{\mu_8},$$

$$b_3 = N_2^2 \nu_i,$$

$$b_2 = H_B^{i*} c_a \nu_i + I_{cr}^* N_2^2 c_a \nu_r + N_2^2 c_a \mu_a - a_3 c_i k_i,$$

$$b_1 = H_B^{*i2} \delta_i (c_a \nu_r I_{cr}^* - a_1 - c_a \mu_a) - \mu - a_0$$

$$+ H_B^{*i} (c_a \nu_i + \zeta k_i c_i I_{cr}^*) + a_3 c_i (k_r I_{cr}^* + k_i C^*),$$

$$b_0 = H_B^{*i} (c_a \mu_a + c_a + c_a \nu_r I_{cr}^* + \zeta c_i k_r I_{cr}^2)$$

$$+ I_{cr}^* H_B^{*i} c_i \zeta (k_c C^* + \mu_i),$$

$$d_5 = a_3 c_i c_a \nu_i k_r,$$

$$d_4 = a_3 c_i I_{ci}^* (k_r + k_i c_a \nu_i)$$

$$+ a_3 c_i c_a \nu_i (k_r N_1^2 \delta_r a_1 a_0 + k_c \mu_i C^*),$$

$$d_3 = c_i c_a \nu_i k_r H_B^{i2*} (a_3 + \delta_r) + a_0 N_1^2 (a_1 \delta_r + c_a \nu_i I_{cr}^*)$$

$$+ a_3 c_i k_i N_1^2 (a_1 \delta_r I_{cr}^* + c_a \nu_i I_{ci}^{*2})$$

$$+ a_3 c_i k_c \mu_i N_1^2 C^* (\delta_r a_1 + c_a \nu_i) + I_{ci}^*,$$

$$d_2 = a_1 c_i k_r \delta_r H_B^{i2*} (a_3 + \delta_r) + a_0 c_a \nu_i H_B^{*i2}$$

$$+ a_3 c_i c_a \nu_i H_B^{*i2} (k_r + k_i I_{ci}^* + k_c \mu_i C^*)$$

$$+ c_i c_a \nu_i \delta_r H_B^{*i2} (k_r I_{ci}^* + k_i I_{ci}^* + k_c C^* + \mu_i),$$

$$d_1 = c_i k_i \delta_r H_B^{*i2} I_{ci}^* (a_1 a_3 + a_1 \delta_r + a_1 c_i c_a \nu_i k_r \delta_r$$

$$+ c_a \nu_i) + H_B^{*i2} I_{ci}^* (a_3 c_i k_c \mu_i C^* + a_0 c_a \nu_i)$$

$$+ a_1 \delta_r H_B^{*i2} (a_0 + c_i k_i \delta_r) + a_3 c_i c_a \nu_i k_i H_B^{*i2} I_{cr}^*$$

$$+ c_i k_c \delta_r H_B^{*i2} C^* (a_1 a_3 \mu_i + c_a \nu_i + a_1 \delta_r),$$

$$d_0 = a_1 c_i \delta_r H_B^{*i2} (k_i + \mu_i + k_c C^*),$$

$$h_1 = c_a (\nu_r I_{cr} + \nu_i I_{ci} + \mu_a),$$

$$h_3 = c_i (k_r I_{cr}^* + k_i I_{ci}^* + k_c C^* + \mu_i),$$

$$k_3 = \frac{\phi_1 I_{cr}^* c}{(H_B^{i*} + c)^2},$$

$$k_6 = \frac{\phi_2 I_{ci}^* c}{H_B^{i*} + c},$$

$$k_8 = \frac{2 N_1 I_{cr}^* H_B^{i2*} (\alpha H_B^{i*} + N_1 I_{cr}^*)}{(H_B^{i2*} + (N_1 I_{cr}^*)^2)^2},$$

$$k_9 = \frac{2 N_2 I_{ci}^* H_B^{i2*} (\alpha_1 H_B^{i*} + N_2 I_{ci}^*)}{(H_B^{i2*} + (N_2 I_{ci}^*)^2)^2},$$

$$k_{16} = \frac{\phi_1 I_{cr}^* + \phi_2 I_{ci}^* C^{\frac{3}{4}} (H_B^{e*} + c - C H_B^{e*})}{(H_B^{e*} + c)^2},$$

$$\begin{aligned}
 k_1 &= -\mu + \zeta + \frac{\phi_1 H_B^{i*}}{H_B^{i*} + c} \\
 &+ \frac{a_3 c_i (2I_{cr}^* k_r + k_i I_{ci}^* + k_c C^* \mu_i) h_3 - c_i k_r (I_{cr}^{2*} a_3 c_i k_r + I_{cr}^* a_3 c_i k_i I_{ci}^* + I_{cr}^* a_3 c_i k_c \mu_i C + a_0)}{h_3^2} \\
 &- \frac{2N_1^2 I_{cr}^*}{(H_B^{i2*} + (N_1 I_{cr}^*)^2)^2} \frac{a_1 + 2c_a I_{cr}^* \nu_r + c_a \nu_i I_{ci}^* + \mu_a h_1 - c_a \nu_r (I_{cr}^* a_1 + c_a I_{cr}^{2*} \nu_r + c_a \nu_i I_{cr}^* I_{ci}^* + \mu_a I_{cr}^*)}{h_1^2}, \\
 k_2 &= -\frac{I_{cr}^* a_3 c_i k_i h_3 + k_i c_i (I_{cr}^{2*} a_3 c_i k_r + I_{cr}^* a_3 c_i k_i I_{ci}^* + I_{cr}^* a_3 c_i k_c \mu_i C + a_0)}{h_3^2}, \\
 k_4 &= \frac{I_{cr}^* a_3 c_i k_c \mu_i h_3 - c_i k_c (a_3 c_i I_{cr}^{2*} k_r + k_i a_3 c_i I_{ci}^* + a_3 c_i k_c \mu_i C^* I_{cr}^* + a_0 I_{cr}^*)}{h_3^2}, \\
 k_5 &= -\mu - \frac{\phi_2 H_B^i}{H_B^i + c} - \frac{2I_{ci}^* k_i a_3 c_i - c_i a_3 I_{cr}^* k_r + a_3 c_i k_c \mu_i C^* + a_0 h_3}{h_3^2} \\
 &+ \frac{c_i k_i (a_3 c_i I_{cr}^* I_{ci}^* k_r + k_i I_{ci}^{2*} a_3 c_i + a_3 c_i k_c \mu_i C^* I_{ci}^* + a_0 I_{ci}^*)}{h_3^2}, \\
 k_7 &= -\frac{a_3 c_i k_c \mu_i I_{ci}^* h_3 - c_i k_c (a_3 c_i I_{cr}^* k_r + k_i a_3 c_i I_{ci}^{2*} + a_3 c_i k_c \mu_i C I_{ci}^* + a_0 I_{ci}^*)}{h_3}, \\
 k_{10} &= \alpha + \alpha_1 - \mu_v - \frac{3\alpha H_B i 2^* (H_B^{i2*} + (N_1 I_{cr}^*)^2 - 2H_B^{i2*} \alpha H_B^{i3*})}{(H_B^{i2*} + (N_1 I_{cr}^*)^2)^2} \\
 &- \frac{3\alpha_1 H_B i 2^* (H_B^{i2*} + (N_2 I_{ci}^*)^2 - 2H_B^{i2*} \alpha H_B^{i3*})}{(H_B^{i2*} + (N_2 I_{ci}^*)^2)^2} - \frac{2N_1 I_{cr}^* H_B^i (H_B^{i2*} + (N_1 I_{cr}^*)^2) - 2H_B^{i*} N_1 I_{cr}^* H_B^{i2*}}{(H_B^{i2*} + (N_1 I_{cr}^*)^2)^2} \\
 &\times \frac{2N_2 I_{ci}^* H_B^i (H_B^{i2*} + (N_2 I_{ci}^*)^2) - 2H_B^{i*} N_2 I_{ci}^* H_B^{i2*}}{(H_B^{i2*} + (N_2 I_{ci}^*)^2)^2}, \\
 k_{11} &= \frac{\delta_r N_1 H_B^{i2*} (H_B^{i2*} + (N_1 I_{cr}^*)^2) - 2N_1 I_{cr}^* (\delta_r N_1 I_{cr}^* H_B^{i2*})}{(H_B^{i2*} + (N_1 I_{cr}^*)^2)^2}, \\
 k_{12} &= \frac{\delta_i N_2 H_B^{i2*} (H_B^{i2*} + (N_2 I_{ci}^*)^2) - 2N_2 I_{ci}^* (\delta_i N_2 I_{ci}^* H_B^{i2*})}{(H_B^{i2*} + (N_2 I_{ci}^*)^2)^2}, \\
 k_{13} &= \frac{2\delta_r N_1 H_B^i I_{cr}^* (H_B^{i2*} + (N_1 I_{cr}^*)^2) - 2H_B^{i*} (\delta_r N_1 I_{cr}^* H_B^{i2*})}{(H_B^{i2*} + (N_1 I_{cr}^*)^2)^2} \\
 &+ \frac{2\delta_i N_2 H_B^i I_{ci}^* (H_B^{i2*} + (N_2 I_{ci}^*)^2) - 2H_B^{i*} (\delta_i N_2 I_{ci}^* H_B^{i2*})}{(H_B^{i2*} + (N_2 I_{ci}^*)^2)^2}, \\
 k_{14} &= \frac{\phi_1 H_B^{e*} C^{\frac{3}{4}}}{H_B^{e*} + c} - \frac{C^* a_3 c_i k_r h_3 - a_3 c_i^2 k_r (C^* k_r I_{cr}^* + c k_i I_{ci}^* + C^* k_c \mu_i) + a_0}{h_3^2}, \\
 k_{15} &= \frac{\phi_2 H_B^{e*} C^{\frac{3}{4}}}{H_B^{e*} + c} - \frac{C^* a_3 c_i k_i h_3 - a_3 c_i^2 k_i (C^* k_r I_{cr}^* + c k_i I_{ci}^* + C^* k_c \mu_i) + a_0}{h_3^2}, \\
 k_{17} &= \frac{3}{4} \left( \pi_c + \phi_1 I_{cr}^* + \phi_2 I_{ci}^* \left( \frac{H_B^{e*}}{H_B^{e*} + c} \right) \right) C^{-\frac{1}{4}} \left( 1 - \left( \frac{C^*}{C_0} \right)^{\frac{1}{4}} \right) + \left( \pi_c + \phi_1 I_{cr}^* + \phi_2 I_{ci}^* \left( \frac{H_B^{e*}}{H_B^{e*} + c} \right) \right) C^{\frac{3}{4}} \\
 &- \frac{\frac{1}{4} C^{-\frac{3}{4}} C_0^{\frac{1}{4}}}{\left( C_0^{\frac{1}{4}} \right)^2} - \frac{a_3 c_i (k_r I_{cr}^* + k_i I_{ci}^* + 2k_c C \mu_i) h_3 - k_c c_i C^* a_3 c_i (k_r I_{cr}^* + k_i I_{ci}^* + C k_c \mu_i) + a_0}{h_3^2}, \\
 k_{18} &= \frac{a_3 c_i k_r h_3 - c_i k_r (a_3 c_i I_{cr}^* k_r + k_i a_3 c_i I_{ci}^{2*} + a_3 c_i k_c \mu_i C^* I_{ci}^* + a_0 I_{ci}^*)}{h_3^2}.
 \end{aligned}$$